European Geothermal Congress 2016
Strasbourg, France, 19-24 Sept 2016

Modeling the properties of two-phase, multi-component geothermal fluid for use in wellbore simulation

Yodha Y. Nusiaputra[1], Alain Dimier[2], Henning Francke[4], Elisabeth Schröder[4], Sarah Herfurth[4], Thomas Kohl[1]

[1] Karlsruhe Institute of Technology, Institute of Applied Geosciences, 76131 Karlsruhe, Germany

[2] European Institute for Energy Research, 76131 Karlsruhe, Germany

[3] Helmholtz Centre Potsdam, GFZ German Research Centre for Geosciences, 14437 Potsdam, Germany

[4] Karlsruhe Institute of Technology, Institute for Nuclear and Energy Technologies, 76344 Eggenstein-Leopoldshafen, Germany

yodha.nusiaputra@kit.edu

Keywords: Neutral interaction; Gas mixture solubility; Equation of state

ABSTRACT

The thermophysical properties of geothermal fluids play an important role for designing the energy conversion system. Geothermal fluid is a multiphase, multicomponent brine, which can be generalized as the system H2O – salt (Na–Ca–K–Mg–Cl-HCO3) – gas (CO2–N2–CH4–H2S). While modeling the phase behavior is crucial . In this work, a three-zone Equation of State model of geothermal fluids is presented with pressure and enthalpy as independent variables. Hence, it is appropriate for two-phase simulation in geothermal reservoirs, wellbores and heat exchangers. Improved gas activity coefficientsare presentedbased on the extension of neutralinteractions of the dissolved gases. The model can be applied to other multi- salt and gas composition which has been achieved through the fusion of binary systems. The validity of the model presented here has been evaluated by using the experimental data from literature and online field-measurements applying pressure, temperature, and ionic-strength range of 0.5 – 50 MPa, 32 – 177 °C, and 0 – 8.1 mol/kgw, respectively. As shown by the validation, the new model can properly reproduce mutual gas solubility of ternary, quaternary mixtures; density, specific heat capacity, and dynamic viscosity of geothermal brine, and show a benefit compared to VLE of geochemical solvers. The developed model can be coupled to any geochemical solvers useful for two-phase, reactive flow simulation of geothermal fluids.

1. INTRODUCTION

Presence of salts and/or non-condensable gases (NCGs) can seriously complicate any geothermal fluid simulation. For instance, by diss-/exsolution of salts and/or NCGs, the density of the geothermal fluid (geofluid) can be significantly affected. Density has a strong influence on the calculated pressure, temperature, and mass flow-rate in geothermal wellbores. Hasan and Kabir (2010) showed consideration of salts and NCGs may also be obligatory to compute accurate pressure and temperature profile along geothermal wells. Consequently, more realistic representations of geothermal fluids must include salts and NCGs. The common independent variables of the properties of salts-water or NCGs-brine are pressure and temperature (p,T). At specified pressure, temperature is approximately constant when water-evaporation occurs. Hence, the thermodynamic state of two-phase fluids has to be defined by specifying another combination of two independent state properties. In fluid simulation, the independent variables are usually pressure and specific enthalpy (p,h). The Equation of State (EoS) described in this study will be based on them. It mainly consists of two models: (1) Vapor-Liquid Equilibrium (VLE) of liquid (aqueous) and gas (non- aqueous) phase (2) thermophysical properties, i.e. density, isobaric heat capacity/enthalpy, dynamic viscosity, and thermal conductivity.

To develop a VLE or gas solubility model, generally two approaches are used, that are fugacity-fugacity (ϕ-ϕ) and fugacity-activity (ϕ-γ). The first approach (ϕ-ϕ) uses one EoS to compute fugacity of all phases in equilibrium, and the equations are solved by fugacity equality of different phases. A recent example of this approach can be found in the work of Li et al. (2015), which is a modification of Soreide and Whitson (1992) model. The model can reproduce experimental data of single-gas brine and gas-mixture brine with good accuracy. Nevertheless, the effect of salts (other than NaCl) which commonly exists in geothermal system has not been included. Pruess and Nicolas (2006) proposed an EoS module for TOUGH2 with the

thermodynamic which handles equilibrium calculations of the system CO2–H2O–NaCl. However, the fugacity of non-aqueous H2S in the fluid is not included in the module. Battistelli (2008) developed TMVOC which was implemented in TOUGHReact (Xu et al., 2007) for modeling mixtures of water, non-condensable gases, volatile organic components and dissolved solids. Furthermore, Battistelli and Marcolini (2009) lately took an important step by presenting the EOS TMGAS coupled into TOUGH2 to model brine and gas mixtures (CO2, H2S and hydrocarbons). The TMGAS model can accurately reproduce the gas–brine equilibrium in wide temperature and pressure range. Nevertheless, for salt molality higher than 2 mol/kg-of-water, the accuracy determined by comparing with the experimental data declines. Salt effect (?)

The fugacity-activity approach, (ϕ-γ) predicts the gas solubility by implementing ideal gas, virial, or cubic, e.g. Peng-Robinson (PR), Soave Redlich Kwong (SRK) equation to compute the non-aqueous phase fugacity, and activity model is used for the calculation of the activity coefficient of the aqueous phase. Equality of chemical potential in both phases yields a system of equations, which is solved to determine the VLE. A recent work based on this approach is presented by Springer et al. (2015) on extension of speciation based model for mixed-solvent electrolyte systems (Wang et al., 2002) to comprise CO2–H2S–NaCl–CaCl2–water system. Unfortunately, in this model and in some other publications, e.g. TMGAS, which are proprietary software, not all details of the EoS have been released. Thus, they are not easily available or reproducible for broader academic investigations in geothermal energy. Appelo (2014) used Peng-Robinson for gas-phase fugacities computation with Henry constants to model the solubility of NCGs which is assembled in PHREEQC, a geochemical speciation solver. However, the upper limit of the validity range is below 200 °C, and validity of H2S solubility has not been clearly presented. Other studies have been conducted by Ziabakhsh-Ganji and Kooi (2012) and Zirrahi et al. (2012) on modeling the CO2–CH4–H2S–brine equilibrium. Nonetheless, the pressure and temperature validity ranges (lower than 60 MPa and 110 °C) ignore geothermal applications of practical attention. Duan Research Group, gave wide-ranging measurement studies for a single gas component solubility in pure water or brine of CO2, N2, CH4 and H2S (Duan and Mao, 2006; Duan and Sun, 2003; Duan et al., 2007; Duan et al., 2006; Mao and Duan, 2006; Mao et al., 2013). But their work does not consider gas mixture solubility which is of more practical significance in actual field applications. (Francke, 2014) has unified these Duan's single-gas solubility functions to model CO2–N2–CH4 mixture solubility. However, the model still considers the gas phase as an ideal gas (fugacity coefficients equal to unity) which tends to fail at higher pressures and for gas with strong intermolecular forces, i.e. water-vapor. While, to calculate the gas solubility, fugacity of single-NCG system is used with sum of water-vapor and NCGs partial pressure as input to the auxiliary functions.

In our work, the VLE model is also based on a fugacity-activity (ϕ-γ) approach, which is less iterative than a fugacity-fugacity approach. The model is based on the EoS for systems of NaCl-KCl-CaCl2–N2–CO2–CH4–H2O presented by Francke (2014). The extension includes Peng-Robinson real-gas equation for fugacity calculation and fusion of Duan Research Group solubility models for each NCG – brine system to model gas-mixture, with total pressure as input to the auxiliary functions since it corresponds to aqueous-phase pressure. This model covers mixture of CO2–N2–CH4–H2S and brine of Na+, K+, Mg2+, Ca2+, Cl-, (HCO3)- to provide accurate thermohydro-chemical simulation as a complementary code to any geochemical solvers, i.e PHREEQC, GEMS.

The thermophysical properties models, i.e. density, isobaric heat capacity/enthalpy, viscosity, and thermal conductivity are already assembled by some workers for a single electrolyte (salt) or seawater. Although, the accurate models of mixed electrolytes (salts) system are mostly available only for density. Francke (2014) describe in detail a model of geofluid thermophysical properties which is limited to NaCl, CaCl2, and KCl. In our work, parameters for other salts, such as MgCl2, NaHCO3, were added. Enhancements on the explicit model for enthalpy and the properties of dissolved-gas, gas (non-aqueous) phase were also carried out.

2. CHEMICAL CHARACTERIZATION OF GEOTHERMAL FLUIDS

During production and injection, geothermal fluid imposed by large variation of pressure and temperature. This pressure-temperature change is strictly connected with the scaling phenomena, causing consequently fouling and damaging of the exchangers, pipings and reinjection wells. The deposition and scaling phenomena can be huge when the temperature decreases. For this reason it is not possible to cool the geothermal fluid at lower temperatures than 70 °C - 50 °C usually, depending on the type of ions and chemicals in the fluid. Moreover, for a correct reinjection strategy, you have to take into account the circulation model of the fluid in the regional area considered. The task is in fact the optimization and the enhancement of the durability of the energy stored in the total volume considered. Also for the reinjection technologies a general methodology is not available, but the optimal strategy is site-dependant, as for the potential assessment itself.

When scaling and deposition of chemicals (present in the geofluid withdrawn) are dominant phenomena, the early study of the "reservoir (rock/fluid) - drilling utilities - power plants" is fundamental, in order to avoid the worst consequences of fouling and corrosion of the parts of the plant, of the pipings, and the "tapping" of the wells. Generally scaling increases when pressure and temperature decrease. High pH let the deposition increase too. The boiling point changes also with the concentration of diluted gases (CO2 in

particular, which is the most present gaseous component in the geofluids of several geothermal fields). The correct project of the equipment for the production test of the wells and the design of the pipings linking the wellheads and the power plant have to take into account these parameters, not to let the pressure drop under critical values.

With current limitation of geochemical solver in gas solubility, i.e PHREEQC. Aim of this study is to complement geochemical solvers with accurate gas mixture solubility model and thermophysical properties for two-phase, reactive flow simulation. Geothermal fluids can be classified as 2Na+/Ca2+–2Cl-, Na+/K+–Cl-, Na+–(HCO3)-, and Na+–Cl-–(HCO3)- types. The amounts of salt associated with (SO4)2- are negligible compared to the ones named before. The characteristic of geothermal fluids worldwide is depicted in Figure 1. It shows the distribution of geothermal resource worldwide with regard to its temperature and total dissolve solids (TDS). Deeper the reservoir, higher the TDS, designating the necessity of such water-salt-gas properties modelling.

In this work, the multicomponent geothermal fluid properties are modeled by using an object-oriented approach, which decomposes the fluid into classes of binary systems, i.e. salts binary systems: NaCl–H2O, CaCl2–H2O, KCl–H2O, MgCl2–H2O, and NCGs binary systems: CO2–brine, N2–brine, CH4–brine, and H2S–brine as can be seen in Figure 2. By using this approach, the model can simply be extended to other salts and NCGs. To exclude critical temperature variation due to bulk fluid composition, we limit the two-phase calculation up to critical temperature of water (374 °C), which is reasonable for extracting process related and not geological origin simulation.

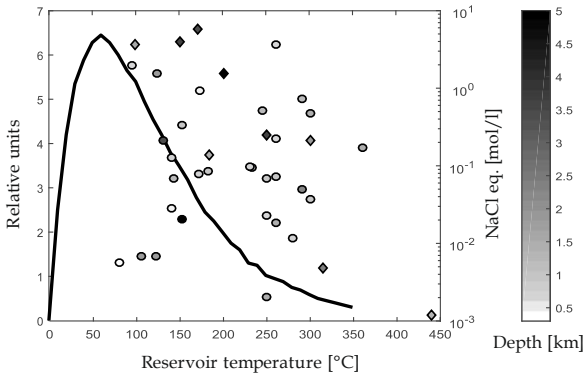

Figure 1: Geothermal fluid characteristic based on temperature and total dissolved solids

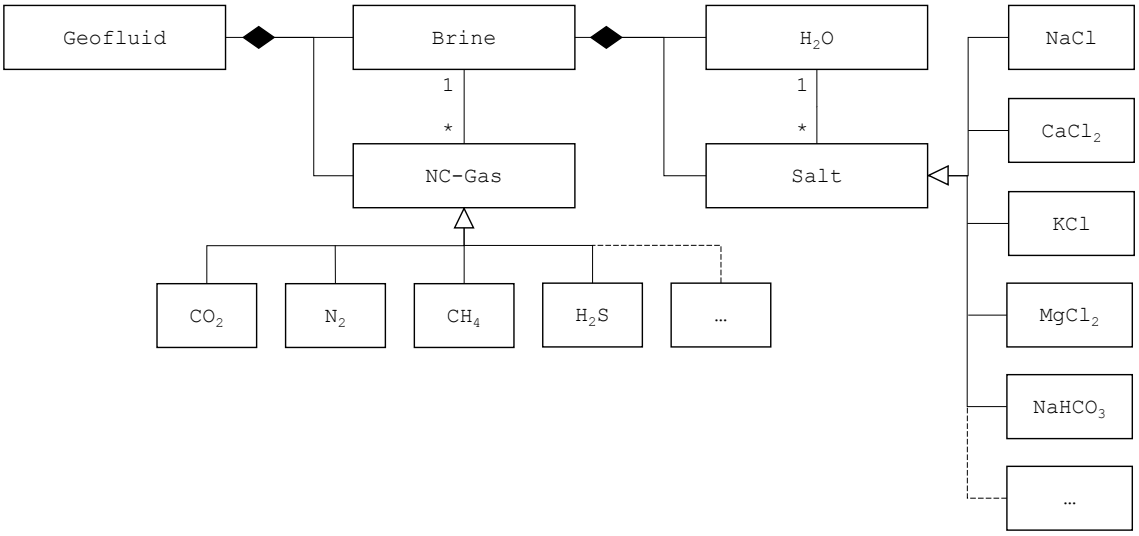

Figure 2: Unified Modeling Language (UML) diagram of the geothermal fluid model

3. THE EVALUATION OF VAPOR-LIQUID EQUIBLIRIUM

3.1 Theoretical background

In this study, a model of vapor-liquid equilibrium has been devised by fusion of gas solubility models by the Duan Research Group. The model combines the Peng-Robinson (PR) equation of state with Duan's semi-empirical equations for the dimensionless standard chemical potential, second-, and third-order (salts-gas) interaction parameters of CO_2, N_2, CH_4, and H_2S. The PR equation is used to calculate the gas mole fractions and its fugacity coefficient, iteratively with the Duan's equations to calculate the gas solubility.

The PR cubic equation for real-gas mixtures is solved to determine the molar volume, V_m, at given pressure and temperature (Peng and Robinson, 1976), and later the fugacity coefficients of each gas component separately, and can be written as

$$p = \frac{RT}{V_m - b_m^*} - \frac{a\alpha_m}{V_m(V_m + b_m^*) + b_m^*(V_m - b_m^*)}, \quad (1)$$

with $a\alpha_m = \sum_j \left(\sum_{j'} \left(y_j y_{j'} \left(a_j \alpha_j \cdot a_{j'} \alpha_{j'}\right)^{0.5}\right)\right)(1 - k_{jj'})$, $b_m^* = \sum y_j b_j^*$, $a_j = 0.45724 \cdot (RT_c)^2/p_c$,

$b_j^* = 0.0778 \cdot RT_c/p_c$. Here, p_c and T_c are the critical pressure and critical temperature of gas j; y_j is the mole fraction of gas j in the non-aqueous mixture, and kjj' are binary interaction parameters for gas pairs, taken from (Soreide and Whitson, 1992). Being a cubic equation, the PR equation has three solutions. For the gas phase, the maximum solution is taken as the molar volume of the mixture. By using the real-gas equation, the compressibility factor can be computed as $Z = PV_m/RT$. Then the fugacity coefficient of gas ϕ_j can be calculated by

$$\begin{aligned}&\ln(\phi_j) \\ &= B_r(Z-1) - \ln(Z-B) \\ &+ \frac{A}{2.828B}\left(\frac{B_r - 2a\alpha_{\mathrm{m},j}}{a\alpha_{\mathrm{m}}}\right)\ln\left(\frac{Z+2.414B}{Z-0.414B}\right),\end{aligned} \tag{2}$$

where $B_r = b_j^*/b_{\mathrm{m}}^*$, $A = a\alpha_{\mathrm{m}}/(RT)^2$, $B = p \cdot b_{\mathrm{m}}^*/RT$. The mole fraction of water vapor is not included in the iterative process of the gas solubility calculation since it was assumed to be $y_{\mathrm{H_2O}} = p_{s,\mathrm{H_2O}}/p$ (ideal mixing). For an ionic strength below the halite saturation, Raoult's Law can be implemented to predict the saturation pressure of water $p_{s,\mathrm{H_2O}}$,

$$\begin{aligned}p_{s,\mathrm{H_2O}} = p^0_{s,\mathrm{H_2O}} &\cdot \left(\frac{w^{AQ}_{\mathrm{H_2O}}}{M_{\mathrm{H_2O}}}\right) \\ &\cdot \left(\frac{w^{AQ}_{\mathrm{H_2O}}}{M_{\mathrm{H_2O}}} + \sum_{N_j} z_j \frac{w_j^{AQ}}{M_j}\right)^{-1},\end{aligned} \tag{3}$$

where $p^0_{s,\mathrm{H_2O}}, w, M, \sum_{N_j} z_j$ are saturation pressure of pure-water, mass fraction, molar mass, and the Van't Hoff factor (sum of the z_j ion valence number).

α_j, is a function of the temperature which is based on the modified version of the generalized expression similar to (Li and Yang, 2013), which was originally developed for water,

$$\begin{aligned}\alpha_j = \Big[1 &+ c_1\left(1 - \tilde{T}_j\right) + c_2\left(1 - \tilde{T}_j^{-1}\right) \\ &+ c_3\left(1 - \tilde{T}_j^{-2}\right)\Big]^2\end{aligned} \tag{4}$$

with $\tilde{T}_j = T/T_c$. The alpha functions for each gas are fitted to Duan's virial functions for single-gas fugacity with relative mean squared error of 0.009. Particular consideration should be taken for H_2S which has a higher critical temperature T_c of 100 °C compared to the other gases. Thus, two different set of constants are used to represent the subcritical and supercritical conditions.

In this work, the binary interaction parameters $k_{jj'}$ for the non-aqueous phase follow the original model by Soreide and Whitson (1992). No interaction parameters between NCGs are considered.

The mole fraction of gases y_j and the calculated fugacity coefficients ϕ_j are then used to compute the gases solubility K_j in mol/kg$_w$, as a function of pressure, temperature, and ionic strength:

$$\begin{aligned}&\ln(K_j) = \ln(y_j \cdot \phi_j \cdot p) - \mu_j^{1(0)}/RT - \\ &2\lambda_{j-\mathrm{Na}}\left(b_{\mathrm{Na^+}} + b_{\mathrm{K^+}} + 2b_{\mathrm{Ca^{2+}}} + 2b_{\mathrm{Mg^{2+}}}\right) - \\ &\xi_{j-\mathrm{Na-Cl}}\left(b_{\mathrm{Na^+}} + b_{\mathrm{K^+}} + c \cdot b_{\mathrm{Ca^{2+}}} + c \cdot\right. \\ &\left. b_{\mathrm{Mg^{2+}}}\right)\left(b_{\mathrm{Cl^-}} + b_{\mathrm{HCO_3^-}}\right) - \sum_{j'} \lambda_{j-j'} \cdot b_{j'}.\end{aligned} \tag{5}$$

$\mu_j^{1(0)}/RT$ is the dimensionless standard chemical potential. $\lambda_{j-\mathrm{Na}}$ and $\xi_{j-\mathrm{Na-Cl}}$ are the second-, and third-order gas-salts interaction parameters. c_1 is 1 for (CO_2, H_2S), and 2 for (N_2, CH_4). These three terms are auxiliary functions with a dependency on total pressure and temperature. The term of $\lambda_{j-j'}$ represents short-range interactions between neutral dissolved gases molecules that are shown in Table 1.

Table 1: Binary parameters used in the short-range interaction term (Eq. (5))

Gas j	Gas j'	$\lambda_{j-j'}$
CO_2	CH_4	-0.5529
CH_4	CO_2	-0.1111
CO_2	H_2S	-0.2217
H_2S	CO_2	0.2121
CH_4	H_2S	-0.1602
H_2S	CH_4	$6.2304 \cdot \ln(x) - 25.92$

After evaluating the solubility, we get the new mole fractions of gases. This is repeated until Eqs. (1) – (5) are fulfilled.

The solubility functions are valid for (1) CO2: 0 – 150 MPa, 0 – 460 °C, and 0 – 4.5 mol/kgw of ionic strength, (2) N2: 0 – 60 MPa, 0 – 317 °C , and 0 – 6 mol/kgw of ionic strength, (3) CH4: 0 – 200 MPa, 0 – 300 °C , and 0 – 6 mol/kgw of ionic strength, (4) H2S: 0 – 100 MPa, 0 – 227 °C , and 0 – 6 mol/kgw of ionic strength. The validity can be extended by fitting parameters to new experimental solubility data of single-gas in water/brine. For instance, the original Duan's function of H2S is only valid up to 21 MPa. However, to cover pressure of practical interest we extended the function of standard-chemical-potential by fitting the parameters to the simulation results from (Springer et al., 2015). The fitted parameters are tabulated in Table 2.

Table 2: Parameters for the H2S standard chemical potential equation by Duan et al. (2007) fitted for 21 MPa < p ≤ 100 MPa.

	$\mu_{H_2S}^{1(0)}/RT$		$\mu_{H_2S}^{1(0)}/RT$
c_1	2.30E+2	c_5	-9.68E+3
c_2	-6.31E-1	c_6	2.38E-3
c_3	-2.45E+4	c_7	-3.10E-1
c_4	7.55E-4	c_8	-1.28E-4

By using mass balance, the main output from the VLE model is the ratio between the non-aqueous phase mass and the total mass,

$$x = \left(m_{H_2O}^{NA} + \sum m_j^{NA}\right) / \left(m_{H_2O} + \sum m_i + \sum m_j^{AQ} + \sum m_j^{NA}\right)$$

3.2 Description of the code

The algorithm used in this study calculates the thermodynamic properties of brine (liquid water with salts), water-vapor and non-condensable gases using the correlations presented in previous section. It covers a wide range of pressure and enthalpy, therefore the p-h domain is divided into three zones: (1) Gas-exsolution (single-phase liquid, non-boiling two-phase of NCG-water) and supercritical zone, (2) water vapor dominated (boiling two-phase with most of NCG has been exsolved), (3) superheated (water-vapor and NCG). The zones (see Figure 3S (Supporting Material)) is numerically partitioned by

$$Zone\ (1):\ h \le h_{\text{exs}}\ ,$$

$$Zone\ (2): h_{\text{exs}} < h \le h_{\text{dry}}\ ,$$

$$Zone\ (3): h > h_{\text{dry}}\ .$$

Boundary functions of h_{exs} is enthalpy at T_{s,H_2O}, where the NCGs has been exsolved, and h_{dry} is enthalpy at $x = 1$. The boundary enthalpies are computed at the initialization. Three different solvers, based on mass balances, were implemented to compute geofluid properties at these zones, which are presented in the following subchapters.

3.2.1 Fugacity-activity solver

The fugacity-activity solver is used for zone 1. The number of unknown variables are reduced to three, namely y_j, x_(H_2 O), and T. Accordingly, a set of three functions, Eqs. (34) are solved in sequence by using iterative method. In this work, the functions are solved by means of the hybrd powell algorithm in Python.

$$f_{11} = y_j - y_{j,\text{new}}, \text{ inner loop}$$

$$f_{12} = \left[\frac{(h-h^{AQ})}{(h^{NA}-h^{AQ})} - x\right] (\text{as function of } T), \quad (6)$$

outer loop

with $x_{H_2O} = m_{H_2O}^{NA}/m_{H_2O}$, n_j is mole quantity of specific component, i.e. j for gas component. The number of variables can be reduced further if we assume the following conditions:

- The molality is constant or the water-vapor mass fraction is $x_{H_2O} \cong 0$. This is valid for temperatures far below the saturation temperature, where the water-vapor fraction is low. By applying that assumption, the intermediate loop (see **Fehler! Verweisquelle konnte nicht gefunden werden.**) can be ignored.
- Temperature is used as an independent variable instead of enthalpy. Hence, the outer loop (see **Fehler! Verweisquelle konnte nicht gefunden werden.**) can be excluded.

The procedure to execute the core routine of the "fugacity-activity" solver (inner loop in **Fehler! Verweisquelle konnte nicht gefunden werden.**) consists of four steps:

1. Determine the input composition (mass fraction) of salts and gases in the geofluid. We need to compute the mole fraction of each gas (in aqueous and non-aqueous phases) under the given condition, i.e. pressure, temperature, salt and gas mass fraction (p, T, w_i, w_j).
2. Initial estimate of mole fraction in the gas phase, y_j. In this step, the water-vapor quality (mass-fraction) is necessary to update the molality of the salts. For unknown variable reduction the mole fraction of water-vapor is calculated by $y_{H_2O} = p_{s,H_2O}/p$, where p_{s,H_2O} is calculated in Eq. (3).
3. Solve the Peng-Robinson cubic equation to compute the compressibility factor, Z, and thus gases fugacity with Eq. (2).
4. Calculate molality of each gas in the aqueous phase $b_{i,\text{new}}$ and its mole fraction in non-aqueous phase $y_{i,\text{new}}$. Update the new value until convergence of $y_j = y_{j,\text{new}}$ achieved, solving f_{11}.

Brine-CO_2-H_2S

All figures and tables (beside the tables A-G at the end of the paper) should In **Fehler! Verweisquelle konnte nicht gefunden werden.**, the simulated CO_2 and H_2S solubilities in electrolyte (CO_2-H_2S-NaCl-H_2O) solution is compared with the experimental measurements from (Bachu and Bennion, 2009) and (Savary et al., 2012), respectively. For the first experiment of the quaternary-mixture, the predicted values of the solubilities has an absolute average relative deviation (AARD) of around 5 %. Thus, the qualitative dependency of the solubility on dry (excluding water-vapor) non-aqueous mole-fractions and pressure can be explained in all cases, e.g. mixture #1: 33 % CO_2, 67 % H_2S; mixture #2: 50 % CO_2, 50 % H_2S; mixture #3: 60 % CO_2, 40 % H_2S. Increasing the non-aqueous gas mole fraction increases the corresponding gas solubility.

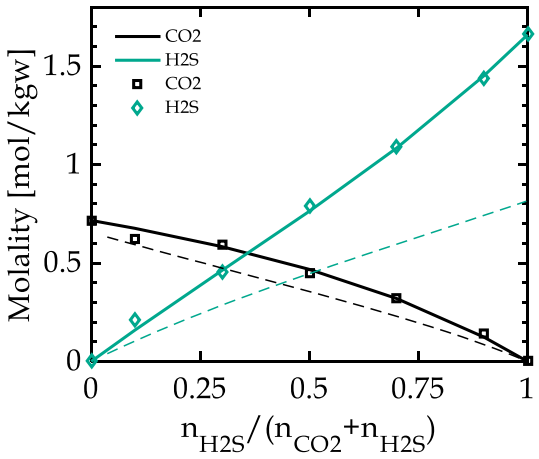

Figure 3: Molality of CO2 and H2S in aqueous phase varying with H2S mole fraction in dry non-aqueous phase: Dots are calculated results from (Bachu and Bennion, 2009), and solid lines are predicted values. The experiment was conducted at p = 13.5 MPa and T = 61 °C, with NaCl concentration of 11.9 % (mass fraction)

Water-CO_2-CH_4

Figure 4 and Figure 5 compares the solubilities of CO2 – CH4 measured and predicted by the model as a function of pressure (Dhima et al., 1999), and as a function of CO2 dry non-aqueous mole-fraction (Qin et al., 2008). In the first experiment of the ternary-mixture, different feeds of CH4−CO2 mixtures were charged in presence of water at temperature of 71 °C and pressures of 10, 20, 50, and 75 MPa, respectively. The CH4 mole fractions in the non-aqueous mixtures have been classified into two groups. The CH4 mole fractions of 0.567, 0.570, 0.585, and 0.587 in non-aqueous mixtures are labeled as mixture #1, while, the CH4 mole fractions of 0.8045, 0.8102, 0.8205, and 0.8260 are labeled as mixture #2. For both CH4 and CO2 at 71 °C, the solubility increases with an increase in pressure. Moreover, it is found that the more CO2 or CH4 is in the dry non-aqueous mixture, the greater the amount of corresponding gas is dissolved in water. In general, the model developed in this work is able to accurately predict the CO2 mole fraction in the aqueous phase of ternary mixture with CH4. The AARD is roughly calculated as 4 %.

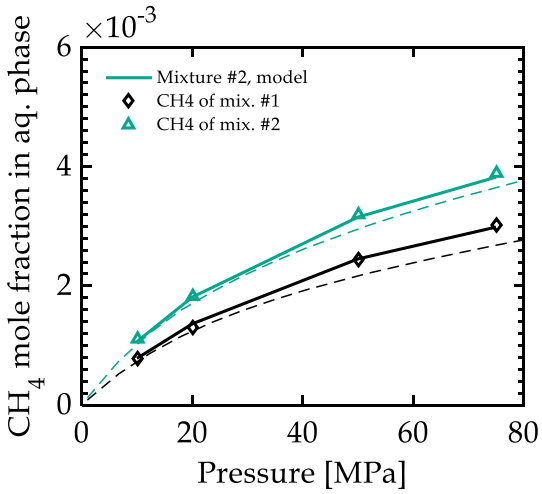

Figure 4: Aqueous mole fraction of CO2 and CH4 varying with pressure: Points are measured values from (Dhima et al., 1999), and predicted values (solid lines). The experiment was conducted at T = 71 °C.

In the second experiment, a similar trend is observed. CO2 solubility decreases with CH4 content and increases with pressure. We observe that the agreement between the measurement and the prediction by the model is very good for CO2 at 103 °C. However, predicted solubility is slightly lower for CH4 (the AARD is around 7 %). Both CO2 and CH4 solubilities are in good agreement at 52 °C, with AARD of approx. 5 %, respectively. In general, the simulation model predicts the qualitative trends of the solubilities, especially for CO2.

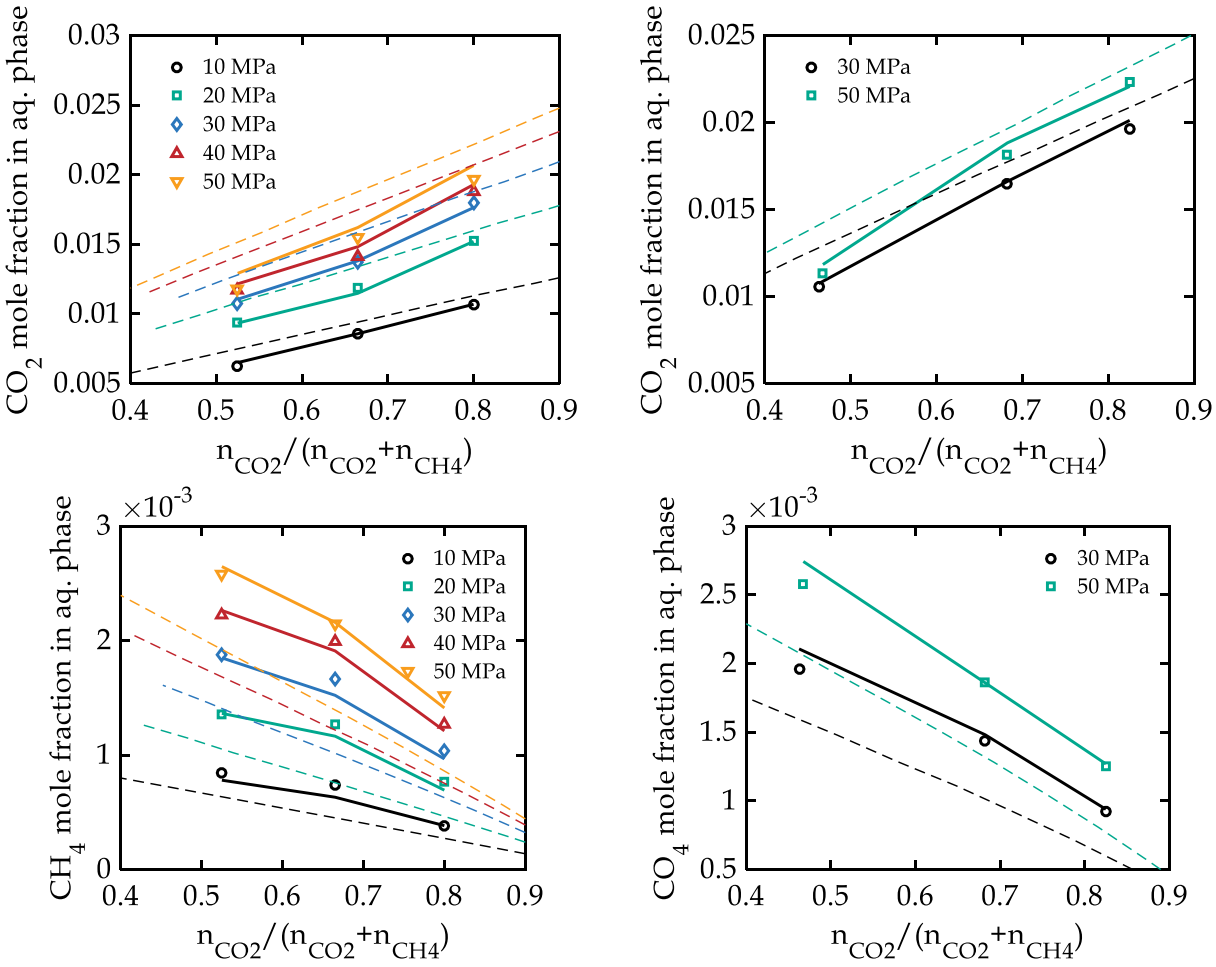

Figure 5: Aqueous mole fraction of CO2 and CH4 varying with CO2 mole-fraction in dry non-aqueous phase: Experimental data from (Qin et al., 2008) (dots) are compared with calculated values (lines).

Water-CO_2-CH_4-H_2S

Huang at al. (1985) measured the phase equilibrium for CO2 – CH4 – H2S – water system, with a feed composition of 30 % CO2, 15 % CH4, 5 % H2S, and 50 % H2O (mole fractions). Figure 7 compares the predicted solubilities with the measured solubilities of the quaternary mixture. The model predicts the CO2 solubility in very good agreement. However, the model seems to slightly underestimate the CH4 solubility and to considerably overestimate H2S solubility for the higher temperatures (107 °C and 177 °C). The AARD is about 12 %. The higher AARD in the quaternary mixture may indicate strong influence of the short-range interactions, ln⁡(γ_j^SR) (see Eq. 3), involving neutral molecules, e.g. dissolved gases (Abrams and Prausnitz, 1975), especially correspond to such polar components as H2S (Ungerer et al., 2004). In general, the dependency of the solubility with respect to pressure, temperature, and composition in aqueous phase can be predicted.

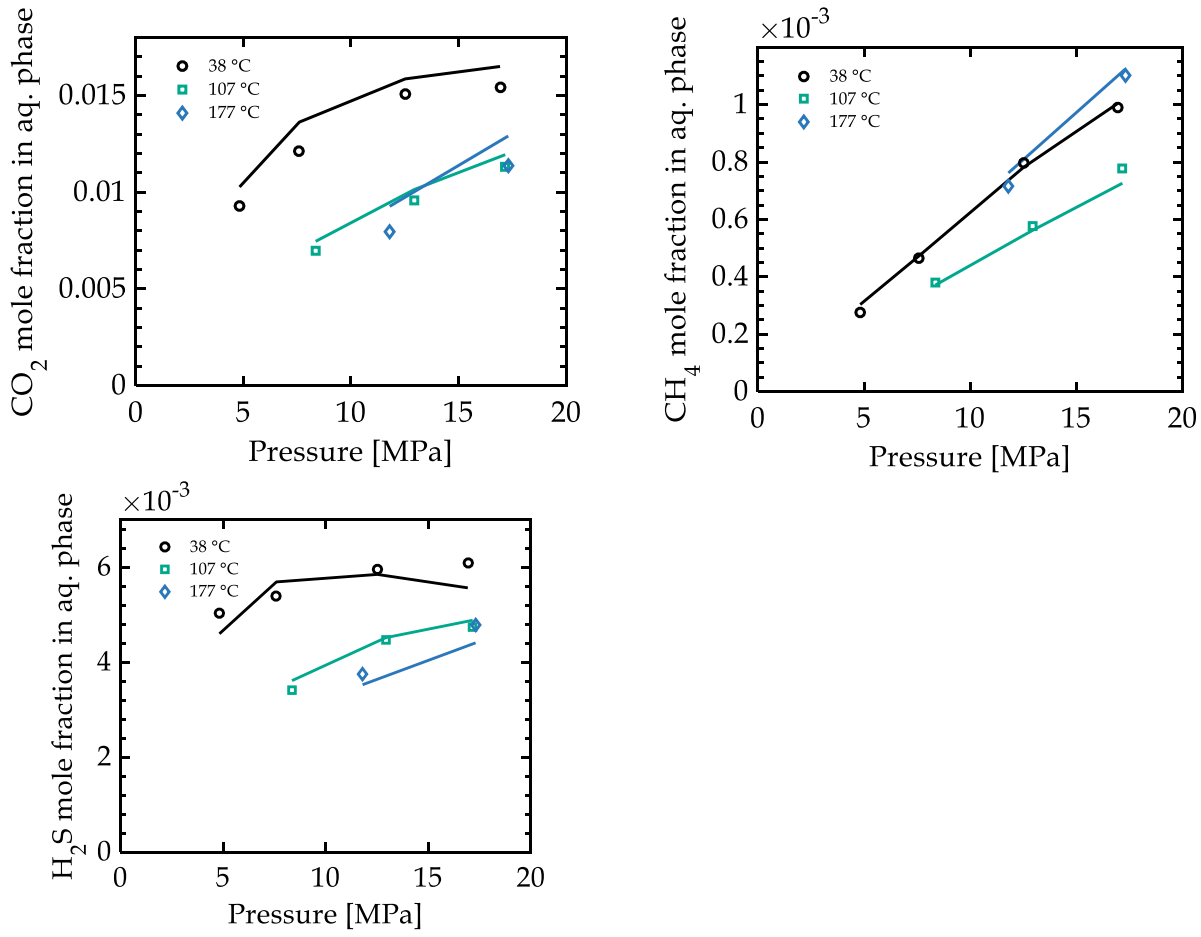

Figure 6: Aqueous phase mole fraction of CO2, CH4, and H2S: Comparison between model results (lines) and measured data from (Huang et al., 1985) (dots) for H2O–CO2–CH4–H2S equilibrium. Feed composition (mole fraction): 50 % H2O, 30 % CO2, 15 % CH4, 5 % H2S.

From these validations, the presented model is reliable to predict gas mixture – water/brine equilibrium. The existing experimental data of geothermal multi-component fluids are still limited and more experimental work is required to enable more comprehensive analysis, particularly regarding the short-range interaction between neutral, dissolved gas molecules.

3.2.2 Water-vapor solver

The water vapor solver is used for zone 2, where water vapor dominates the non-aqueous phase. Two variables need to be solved, namely temperature T and water-vapor quality x_(H_2 O). Both variables have to be solved simultaneously since x_(H_2 O) affects salt molality which depends on the amount of evaporation, determined by temperature of the saline-water. This problem is defined in the functions below.

$$f_{21} = T - T_{s,\mathrm{H_2O}}\,, \tag{7}$$

$$f_{22} = x_{\mathrm{H_2O}} - \frac{(h - h^{\mathrm{AQ}})/(h^{\mathrm{NA}} - h^{\mathrm{AQ}}) \cdot \left(m_{\mathrm{H_2O}} + \sum m_i + \sum \right.}{m_{\mathrm{H_2O}}}$$

with $T_{s,\mathrm{H_2O}}$ saturation temperature of water, m mass; i is index for salt components, and j for NCG components.

3.2.3 Vapor-gas solver

The vapor-gas solver is used for zone 3, where water has been fully evaporated. One variable has to be solved for zone 3 which is temperature T. The function is defined by

$$f_{31} = h - h^{NA}(T)\,. \tag{8}$$

After solving the VLE, which yields temperature T and non-aqueous phase quality x, the effective thermophysical properties of the geofluid can be evaluated, i.e. density ρ, specific heat capacity c_p, viscosity η, and thermal conductivity λ.

4. THE THERMOPHYSICAL PROPERTIES OF THE MIXTURES

It is always helpful to summarise your findings and present them in a conclusion chapter. After this chapter, list the references, and check that all literature listed is actually cited in the text. The references should follow the style shown below.

4.1 Isobaric heat capacity and enthalpy

The effective specific heat capacity of the two-phase geofluid c_p is evaluated using a mass-average-mixture specific heat capacity,

$$c_p = (1 - x) \cdot c_p^{AQ} + x \cdot c_p^{NA} \,. \tag{9}$$

The specific heat capacity of the gas-mixture c_p^{NA} is determined by using GERG 2008 EoS by using the mixing correlation by Kunz and Wagner (2012) e.g. via CoolProp (Bell et al., 2014) (CoolProp). In addition, by analogy to Eq. (16), the specific heat capacity of the aqueous phase c_p^{AQ} can be expressed with the specific heat capacity of water and the apparent molar heat capacities of the particular salts, and is written as

$$c_p^{AQ} = w_{\mathrm{H_2O}}^{AQ} \cdot c_{p,\mathrm{H_2O}}^{AQ} + \sum_{N_i} \frac{w_i^{AQ}}{M_i} \cdot c_{p,i}^{\phi} + \sum_{N_j} \frac{w_j^{AQ}}{M_j} \cdot c_{p,j}^{\phi} \,, \tag{10}$$

where the apparent molar heat capacity, c_p^{ϕ}, is defined as the change of absolute heat capacity of an arbitrary amount of solution caused by the addition of a salt (index i) and gas, (index j). Francke (2014) provided equation Eq. **Fehler! Verweisquelle konnte nicht gefunden werden.** and the coefficients for $CaCl_2$ and KCl apparent heat capacities valid for p = 2.1 – 17.8 MPa, T = 34 – 329 °C, b_{NaCl} = 0.1 – 3 mol/kg$_w$ and p = 16.4 – 17.8 MPa, T = 52 – 327 °C, b_{NaCl} = 0.1 – 3 mol/kg$_w$, respectively. The apparent heat capacity for $MgCl_2$ is extended by fitting experimental data from (White et al., 1988) (from the range: p = 2.3 – 17.9 MPa, T = 76 – 325 °C, $b_{\mathrm{MgCl_2}}$ = 0 – 2.3 mol/kg$_w$).

Increasing salinity decreases mass-specific heat capacity. **Fehler! Verweisquelle konnte nicht gefunden werden.** also shows good agreement between predicted and experimental values for URG-2, MB-1, and MB-2. The accuracy of the model is within 2 %. For Groß-Schönebeck fluid (Na/Ca-Cl), the specific heat capacity decreases up to 23 % compared to pure water. Followed by fluids from Salton Sea #11 (Na/Ca-Cl) and Neustadt-Glewe (Na-Cl). It is interesting to note, that $CaCl_2$ has substantial influence on decreasing specific heat capacity, changing the order compared to the density behavior.

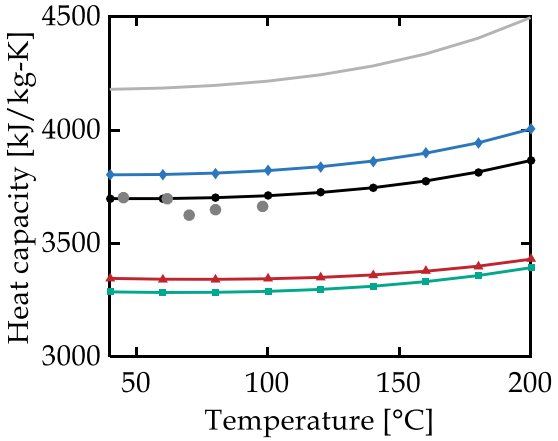

Figure 7: Aqueous isobaric heat capacity. Dots are measured values.

In order to calculate all the properties in the model presented here, where pressure and enthalpy are the independent variables, an additional function for the enthalpy has to be included, which can then be inverted in the common case that temperature is given instead of enthalpy. The specific enthalpy of the two-phase geofluid h can be calculated by analogy to Eq. (9) as

$$h = (1 - x) \cdot h^{AQ} + x \cdot h^{NA} \,, \tag{11}$$

where the enthalpy of gas-mixture in the non-aqueous phase h^{NA} is determined by GERG 2008 via Refprop/CoolProp. To calculate the enthalpy in the aqueous phase h^{AQ} the following formula is used

$$h^{AQ} = w_{\mathrm{H_2O}}^{AQ} \cdot h_{\mathrm{H_2O}}^{AQ} + \sum_{N_i} \frac{w_i^{AQ}}{M_i} \cdot h_i^{\phi} + \sum_{N_j} w_j^{AQ} \left(h_j + \frac{h_{\mathrm{sol},j}^{\phi}}{M_j} \right). \tag{12}$$

$h_{\mathrm{H_2O}}^{AQ}$, h_i^{ϕ} are and the liquid pure-water enthalpy and the apparent molar enthalpy of salt i, respectively. Since we don't have apparent molar enthalpy for dissolved gas, the enthalpy of dissolved gas is estimated by mixing two properties h_j and $h_{sol,j}^{\phi}$, which are the enthalpy of gas j at corresponding total-pressure and the solution enthalpy of gas j. The experimental data for enthalpy of salt solutions are very limited. However, by using the relation between specific heat capacity and enthalpy, enthalpy can be quickly derived from the equation of specific heat capacity by Driesner (2007). The Driesner's equation scales the NaCl solution properties to the pure water properties by scaling the temperature: $h^{NA}(T^*) = h_{\mathrm{H_2O}}^{\mathrm{AQ}}(T_h^*)$, which leads to $c_p^{\mathrm{AQ}}(T) = q_2 \cdot c_{p,\mathrm{H_2O}}^{\mathrm{AQ}}(T_h^*)$. By taking the temperature integral according to the reverse chain rule one can define for any salt i,

$$h_{i,Dr}^{AQ}(p, T, m_i) = \int c_{p,i}^{AQ}(p, T, m_i) \cdot dT$$

$$= \int q_2 \cdot c_{p,\mathrm{H_2O}}^{AQ}\left(T_h^*(p,T,m_i)\right) \cdot dT$$

$$= h_{\mathrm{H_2O}}^{AQ}(p,T_h^*) + c\,, \qquad (13)$$

with $T_h^* = q_1 + q_2 \cdot T$. By setting the integration constant c equal to zero, that equation follows the formulation of Driesner's model. The apparent temperature T_h^* thus can be derived by fitting the experimental data of specific heat capacity of any salts $c_{p,i}^{AQ}$ to Driesner's model of specific heat capacity $c_{p,\mathrm{H_2O}}^{\mathrm{AQ}}(T_h^*)$. Accordingly, after knowing T_h^* we are able to calculate the enthalpy $h_{i,Dr}^{AQ}$. However, the experiments were conducted at constant pressure, while the parameters q_1 and q_2 are strongly pressure dependent. In order to minimize the error, the apparent molar enthalpy h_i^{ϕ} is derived from the calculated enthalpy $h_{i,Dr}^{AQ}$,

$$\begin{aligned} h_i^{\phi} = {} & (c_{01} + c_{02} \cdot b_i + c_{03} \cdot (T + 273.15) \\ & + c_{04} \cdot (T + 273.15)^2) \\ & + \left(b_i^{c_1} + c_2\right) \\ & \cdot \Bigg(c_3 \cdot (T + 273.15) - c_4 \\ & \cdot \ln\left(1 - \frac{T + 273.15}{c_5}\right)\Bigg), \end{aligned} \qquad (14)$$

which considers limited effect of pressure. The parameters for each salts, $c_{01} - c_{04}$ and $c_1 - c_5$, are summarized in **Fehler! Verweisquelle konnte nicht gefunden werden.**. For NaCl, the apparent molar enthalpy is directly calculated from Driesner's model (validity: p = 0.1 – 500 MPa, T = 0 – 1000 °C, NaCl mole fraction of 0 – 1). The fitted data ranges for $CaCl_2$, KCl, and $MgCl_2$ apparent molar enthalpies are similar to those used in fitting the apparent molar heat capacities.

4.2 Density

The effective density of a two-phase mixture can be computed using void fraction, or the ratio, ε, between the non-aqueous phase volume and the total-volume,

$$\rho = (1 - \varepsilon) \cdot \rho^{AQ} + \varepsilon \cdot \rho^{NA}\,, \qquad (15)$$

with ρ^{AQ} and ρ^{NA} denote the density of aqueous and non-aqueous phases, respectively. The density of gas-mixture in the non-aqueous phase ρ^{NA} are calculated using the PR.

The evaluation of the mixed-electrolyte brine (aqueous phase) ρ^{AQ} density was the subject of several previous investigations. A comprehensive density function for a (binary) sodium chloride aqueous solution was developed by Driesner (2007). It is valid for mole fraction of NaCl from 0 to 1 (pure water to halite), pressure and temperature of 0.1 – 500 MPa and 0 – 1000 °C. In addition, Mao and Duan (2008) described different binary aqueous chloride solutions which applied at range of pressure and temperature of 0.1 – 100 MPa and 0 – 300 °C. The mixing rule that converts the apparent molar volume ,V_{ϕ}, to brine density, ρ^{AQ}, is provided by Laliberté and Cooper (2007) as recommended by Francke (2014). It is equivalent to averaged apparent molar-volume, weighted by mole number, Young's rule (Young and Smith, 1954), which is suggested by Zezin et al. (2014). In these methods, the salts' respective apparent molar volumes V^{ϕ} are combined to yield the density of the solution, which can be written as

$$\rho^{AQ} = \left(\frac{w_{\mathrm{H_2O}}^{AQ}}{\rho_{\mathrm{H2O}}} + \sum_{N_i} \frac{w_i^{AQ}}{M_i} \cdot V_i^{\phi} + \sum_{N_j} \frac{w_j^{AQ}}{M_j} \cdot V_j^{\phi} \right)^{-1} \qquad (16)$$

where w is the mass-fraction, i as index for salt components, and j for NCG components.

The main salt constituents in geothermal fluid, i.e. NaCl, $CaCl_2$, KCl, and $MgCl_2$ are considered here. The density of pure water used in this approach is provided by the IAPWS-97 standard (IAPWS, 2007) via Refprop/CoolProp.

Fehler! Verweisquelle konnte nicht gefunden werden. shows the density model is in good agreement with the experimental data as the predicted values lie within the error bars of 1 %. Increasing the salinity increases the density of brine. For the Groß-Schönebeck fluid, it results in a variation up to 18 % higher than the one of pure water. Followed by fluids from Neustadt-Glewe and Salton Sea #11. The lowest density fluids belong to MB-1, MB-2, and Kizildere fluids which are more or less equal to pure water.

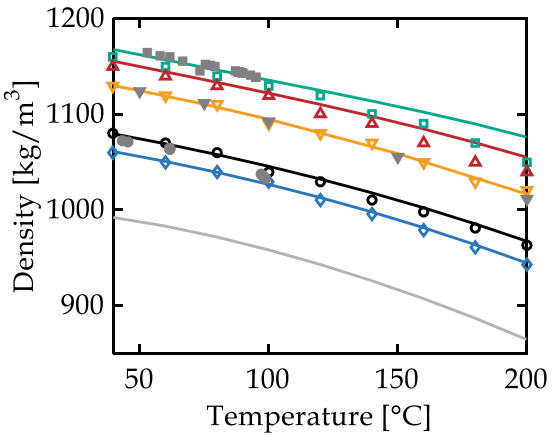

Figure 8: Aqueous phase density. Dots are measured values.

The influence of the dissolved gases, if present, on the brine density is an offset by roughly 2.5 % at mole fraction of 0.05. The correlation for apparent volume of NCGs was based on experimental data from (Hnědkovský et al., 1996). The apparent molar volume is fitted by superposition:

$$V_j^{\phi} = g_1 \cdot f_1 + g_2 \cdot (1 - f_1) + f_2 \quad (17)$$

of two polynomial functions: $g_1(T)$, $g_2(T)$ (in cm^3/mol).

4.3 Viscosity

The effective dynamic viscosity of a two-phase mixture is derived by analogy to effective thermal conductivity using the arithmetic mean of the Maxwell-Eucken 1 and Maxwell-Eucken 2 models (Hashin and Shtrikman, 1962). The model provided good approximation in predicting friction factor in circular tubes (Awad and Muzychka, 2008); it can be expressed by

$$\eta = \frac{1}{2}\left[\eta^{AQ}\frac{2\eta^{AQ} + \eta^{NA} - 2(\eta^{AQ} - \eta^{NA})\cdot x}{2\eta^{AQ} + \eta^{NA} + (\eta^{AQ} - \eta^{NA})\cdot x} + \eta^{NA}\frac{2\eta^{NA} + \eta^{AQ} - 2(\eta^{NA} - \eta^{AQ})(1-x)}{2\eta^{NA} + \eta^{AQ} + (\eta^{NA} - \eta^{AQ})(1-x)}\right] \quad (18)$$

The dynamic viscosity of the aqueous phase η^{AQ} is computed by combining viscosities of binary solutions using a logarithmic mixing rule weighted by molar fraction, as recommended by Francke (2014). It can be written as

$$\eta^{AQ} = \eta^{AQ}_{H_2O} \cdot \prod_{N_i} \eta_{r,i}^{\left(\frac{b_i}{\sum b_i}\right)}, \quad (19)$$

where the viscosity of the binary solutions is expressed by relative viscosity $\eta_{r,i}$ the viscosity ratio of solution and pure water. It was taken from correlations available in the literature, i.e. NaCl, KCl (Mao and Duan, 2009) (validity of p = 0.1 – 100 MPa, T = 0 – 350 °C, b_{NaCl} = 0 – 6 mol/kg$_w$, b_{KCl} = 0 – 4.5 mol/kg$_w$), $CaCl_2$ and $MgCl_2$. The $CaCl_2$ correlation from (Zhang et al., 1997) is based on molarity which is density dependent. Thus, for a simplification purpose, the correlation was converted to a form following (Mao and Duan, 2009), Eq. **Fehler! Verweisquelle konnte nicht gefunden werden.**, (fitted-data range: p = 0.1 – 30 MPa, T = 25 – 300 °C, b_{CaCl_2} = 0.2 – 2.2 mol/kg$_w$). Additionally, a correlation for $MgCl_2$ was derived by fitting to experimental data from Azizov (1999) to the Eq. **Fehler! Verweisquelle konnte nicht gefunden werden.** (fitted-data range: p = 10 – 30 MPa, T = 25 – 300 °C, b_{MgCl_2} = 0.2 – 0.9 mol/kg$_w$):

Fehler! Verweisquelle konnte nicht gefunden werden. compares the viscosity model with three sets of online measurement data from URG-2, MB-1, and MB-2. The difference between predicted and measured values is within 2 % as shown by the error bars. Similar to density, salinity has a proportional effect on viscosity. Here, the effect is much bigger. Groß-Schönebeck and Neustadt-Glewe fluids show an increase of up to 95 % compared to that of pure water, which will have significant impact in any thermo-hydraulic simulation. In contrast, the viscosity of MB-1, MB-2, and Kizildere fluids appear to be similar to pure water.

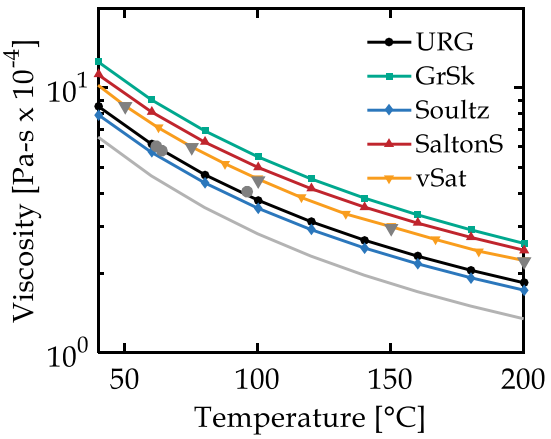

Figure 9: Aqueous viscosity. Dots are measured values.

The non-aqueous phase dynamic viscosity η^{NA} estimation, is based on transport property in Refprop/CoolProp. Nonetheless, the Refprop/CoolProp cannot handle transport equation of water-vapor/gas mixture with water molarity greater than 2 %. Hence, the viscosity is modeled as binary mixture of water vapor and NCGs at the corresponding molar fractions y_{H_2O} and $y_{NCG} = 1 - y_{H_2O}$, respectively. It is calculated based on earlier investigations by Lohrenz et al. (1964), where Novak (2013) showed good accuracy of this equation to predict viscosity of natural gas mixture.

The mixing rule has been validated against calculated moist-air (N_2-O_2-Ar-CO_2-H_2O) dynamic viscosity from ASHRAE-RP1485 by Herrmann et al. (2009). It yields average an absolute relative deviation (AARD) of 0.6 % at the corresponding pressures of 0.1 – 10 MPa, temperatures of 80 – 300 °C, and relative humidity from 0 to 1.

4.4 Thermal conductivity

The effective two-phase thermal conductivity, like dynamic viscosity, is derived by effective thermal conductivity using arithmetic mean of the Maxwell-Eucken 1 and Maxwell-Eucken 2 models (Hashin and Shtrikman, 1962).

The thermal conductivity of the aqueous phase λ^AQ is calculated using the water model by (IAPWS, 2007) which can be retrieved from Refprop/CoolProp. Ignoring the salinity has insignificant effect due to the weak salinity dependence of λ compared to c_p, as investigated earlier by Yusufova et al. (1975).

As of viscosity, the non-aqueous phase thermal conductivity λ^NA is a transport property which cannot be handled by Refprop/CoolProp if the water-vapor molarity exceeds 2 %. Hence, it was regarded as binary mixture of water vapor and NCGs. Kohl and Wagner (2014) suggested the mixing rule used, which was originally proposed for gas-mixtures by Wassiljewa (1904).

5. CONCLUSIONS

In this work, we developed a pressure-enthalpy based three-zone EoS for geothermal fluids by merging the EoS of H2O-salts (NaCl, KCl, MgCl2, CaCl2, NaHCO3) binary and brine-NCG (CO2, N2, CH4, H2S) systems. We presented an easily extendable or adaptable EoS, which is computationally efficient compared to fugacity-fugacity and molecular approach, while maintaining precision and performance as in a simple polynomial approach. The validation of thermophysical properties of water, salts, NCGs, and the mixing rules were based on a comprehensive literature review for the appropriate selection of the most widely accepted procedures and methods.

The built-in functions in the model cover the range of pressure, temperature, and salt molality up to 60 MPa, 227 °C, 4.5 mol/kgw for the system CO2–N2–CH4–H2S–brine; 100 MPa, 227 °C, 4.5 mol/kgw for the system CO2–H2S–brine; 150 MPa, 300 °C, 4.5 mol/kgw for the system CO2–CH4–brine. These validity ranges are sufficient for mid-enthalpy geothermal reservoir, wellbore, and heat exchangers simulation. For a simplified model of the system CO2–H2O–NaCl, the model is valid up to 150 MPa, 460 °C, ∞ mol/kgw (halite) which is suitable for very high-enthalpy applications, e.g. supercritical reservoirs.

The EoS model has been validated using a complete dataset of the VLE and thermophysical properties of geofluids in the temperature range of 32 – 177 °C under total pressures of 0.5 – 50 MPa, which are typical conditions for geothermal applications. For the Vapor Liquid Equilibrium (VLE) between the aqueous and the non-aqueous phases, the Absolute Average Relative Deviation (AARD) of the modeled and the measured values ranges between about 5 % and less than 8 %. The implementation of short-range interaction between neutral, dissolved gas molecules is proposed to improve the VLE prediction accuracy, particularly for large multicomponent mixtures involving polar components such as H2S. For the thermophysical properties of the brine, the AARD is 1 – 2 %. Based on these comparisons, the modeling results are in good quantitative and qualitative agreement with experimental data, confirming the validity of this approach. Hence, the model can be called to any geochemical solver useful for accurate two-phase, reactive flow simulation.

REFERENCES

Abrams, D.S., Prausnitz, J.M., 1975. Statistical Thermodynamics of Liquid Mixtures. A New expression for the Excess Gibbs Energy of Partly or Completely Miscible Systems. AIChe Journal 21, 116-128.

Appelo, C.A.J., Parkhurst, D.L., Post, V.E.A., 2014. Equations for calculating hydrogeochemical reactions of minerals and gases such as CO_2 at high pressures and temperatures. Geochimica et Cosmochimica Acta 125, 49-67.

Awad, M.M., Muzychka, Y.S., 2008. Effective property models for homogeneous two-phase flows. Experimental Thermal and Fluid Science 33, 106-113.

Azizov, N.D., 1999. The main results of investigation of the viscosity of aqueous solutions of electrolytes. TVT 37, 404–410.

Bachu, S., Bennion, D.B., 2009. Chromatographic partitioning of impurities contained in a CO_2 stream injected into a deep saline aquifer: Part 1. Effects of gas composition and in situ conditions. International Journal of Greenhouse Gas Control 3, 458-467.

Battistelli, A., 2008. Modeling Multiphase Organic Spills in Coastal Sites with TMVOC V.2.0. Vadose Zone 7, 316–324.

Battistelli, A., Marcolini, M., 2009. TMGAS: A new TOUGH2 EOS module for the numerical simulation of gas mixtures injection in geological structures. International Journal of Greenhouse Gas Control 3, 481-493.

Bell, I.H., Wronski, J., Quoilin, S., Lemort, V., 2014. Pure and Pseudo-pure Fluid Thermophysical Property Evaluation and the Open-Source Thermophysical Property Library CoolProp. Industrial & Engineering Chemistry Research 53, 2498-2508.

Dhima, A., Hemptinne, J.-C.d., Jose, J., 1999. Solubility of Hydrocarbons and CO_2 Mixtures in Water under High Pressure. Industrial & Engineering Chemistry Research 38, 3144 - 3161.

Driesner, T., 2007. The system H2O–NaCl. Part II: Correlations for molar volume, enthalpy, and isobaric heat capacity from 0 to 1000°C, 1 to 5000bar, and 0 to 1 XNaCl. Geochimica et Cosmochimica Acta 71, 4902-4919.

Duan, Z., Mao, S., 2006. A thermodynamic model for calculating methane solubility, density and gas phase composition of methane-bearing aqueous fluids from 273 to 523K and from 1 to 2000bar. Geochimica et Cosmochimica Acta 70, 3369-3386.

Duan, Z., Sun, R., 2003. An improved model calculating CO_2 solubility in pure water and aqueous NaCl solutions from 273 to 533 K and from 0 to 2000 bar. Chemical Geology 193, 257– 271.

Duan, Z., Sun, R., Liu, R., Zhu, C., 2007. Accurate Thermodynamic Model for the Calculation of H_2S Solubility in Pure Water and Brines. Energy & Fuels 21, 2056-2065.

Duan, Z., Sun, R., Zhu, C., Chou, I.M., 2006. An improved model for the calculation of CO_2 solubility in aqueous solutions containing Na+, K+, Ca2+, Mg2+, Cl−, and SO42−. Marine Chemistry 98, 131-139.

Feldbusch, E., Regenspurg, S., Banks, J., Milsch, H., Saadat, A., 2013. Alteration of fluid properties during the initial operation of a geothermal plant: results from in situ measurements in Groß Schönebeck. Environmental Earth Sciences 70, 3447-3458.

Francke, H., 2014. Thermo-hydraulic model of the two-phase flow in the brine circuit of a geothermal power plant, Fakultät III-Prozesswissenschaften. Technischen Universität Berlin, Berlin.

Garcia, J.E., 2001. Density of aqueous solutions of CO_2. Lawrence Berkeley National Laboratory.

Haklidir, F.T., Sengun, R., Haizlip, J.R., 2015. The Geochemistry of the Deep Reservoir Wells in Kizildere, World Geothermal Congress, Melbourne.

Harting, P., May, F., Schütze, H., 1982. Tabellen und Diagramme zur Löslichkeit von Methan-Stickstoff-Gemischen in wäßrigen Natriumchloridlösung. Akademie der Wissenschaften der DDR, Zentralinst. für Isotopen- u. Strahlenforschung, Leipzig.

Hasan, A.R., Kabir, C.S., 2010. Modeling two-phase fluid and heat flows in geothermal wells. Journal of Petroleum Science and Engineering 71, 77-86.

Hashin, Z., Shtrikman, S., 1962. A Variational Approach to the Theory of the Effective Magnetic Permeability of Multiphase Materials. Journal of Applied Physics 33, 3125.

Herrmann, S., Kretzschmar, H.-J., Gatley, D., 2009. Thermodynamic Properties of Real Moist Air, Dry Air, Steam, Water, and Ice (RP-1485). HVAC&R Research 15, 961-986.

Hnědkovský, L., Wood, R.H., Majer, V., 1996. Volumes of aqueous solutions of CH_4, CO_2, H_2S and NH_3 at temperatures from 298.15 K to 705 K and pressures to 35 MPa. J. Chem Thermodynamics 28, 125 - 142.

Hnědkovský, L., Wood, R.H., Majer, V., 1997. Apparent molar heat capacitites of aqueous solutions of CH_4, CO_2, H_2S, and NH_3 at temperatures from 304 K to 704 K at a pressure of 28 MPa. J. Chem Thermodynamics 29, 731 - 747.

Huang, S.S.S., Leu, A.D., Ng, H.J., Robinson, D.B., 1985. The phase behavior of two mixtures of methane, carbon dioxide, hydrogen sulfide, and water. Fluid Phase Equilibria 19, 21-32.

IAPWS, 2007. Revised Release on the IAPWS Industrial Formulation 1997 for the Thermodynamic Properties of Water and Steam.

Kohl, C.-D., Wagner, T., 2014. Gas Sensing Fundamentals, 1 ed. Springer-Verlag Berlin Heidelberg.

Kuhn , M., Niewohner, C., Isenbeck-Schroter, M., Schulz, H.D., 1997. Determination of major and minor constituents in anoxic thermal brines of deep sandstone aquifers in Northern Germany. Wat. Res. 32, 265-274.

Kunz, O., Wagner, W., 2012. The GERG-2008 Wide-Range Equation of State for Natural Gases and Other Mixtures: An Expansion of GERG-2004. Journal of Chemical & Engineering Data 57, 3032-3091.

Laliberté, M., Cooper, W.E., 2007. Model for calculating the viscosity of aqueous solutions. J. Chem. Eng. Data 52, 321–335.

Lemmon, E.W., Huber, M.L., McLinden, M.O., 2013. NIST Standard Reference Database 23: Reference Fluid Thermodynamic and Transport Properties-REFPROP, Version 9.1, 9.1 ed. U.S. Department of Commerce, Gaithersburg, Maryland.

Li, J., Wei, L., Li, X., 2015. An improved cubic model for the mutual solubilities of CO_2–CH_4–H_2S–brine systems to high temperature, pressure and salinity. Applied Geochemistry 54, 1-12.

Li, X., Yang, D., 2013. Determination of Mutual Solubility between CO_2 and Water by Using the Peng–Robinson Equation of State with Modified Alpha Function and Binary Interaction Parameter. Industrial & Engineering Chemistry Research 52, 13829-13838.

Lohrenz, J., Bray, B.G., Clark, C.R., 1964. Calculating viscosities of reservoir fluids from their composition. J. Pet. Technology 16.

Mao, S., Duan, Z., 2006. A thermodynamic model for calculating nitrogen solubility, gas phase composition and density of the N_2–H_2O–NaCl system. Fluid Phase Equilibria 248, 103-114.

Mao, S., Duan, Z., 2008. The P,V,T,x properties of binary aqueous chloride solutions up to T = 573 K and 100MPa. The Journal of Chemical Thermodynamics 40, 1046-1063.

Mao, S., Duan, Z., 2009. The Viscosity of Aqueous Alkali-Chloride Solutions up to 623 K, 1,000 bar, and High Ionic Strength. International Journal of Thermophysics 30, 1510-1523.

Mao, S., Zhang, D., Li, Y., Liu, N., 2013. An improved model for calculating CO_2 solubility in aqueous NaCl solutions and the application to CO_2–H_2O–NaCl fluid inclusions. Chemical Geology 347, 43-58.

Novak, L.T., 2013. Predicting Natural Gas Viscosity with a Mixture Viscosity Model for the Entire Fluid Region. Industrial & Engineering Chemistry Research 52, 16014-16018.

Peng, D.-Y., Robinson, D.B., 1976. A New Two-Constant Equation of State. Industrial & Engineering Chemistry Fundamentals 15, 59-64.

Pruess, K., Nicolas, S., 2006. ECO2N - A New TOUGH2 Fluid Property Module for Studies of CO_2 Storage in Saline Aquifers, TOUGH Symposium, Berkeley, CA.

Qin, J., Rosenbauer, R.J., Duan, Z., 2008. Experimental Measurements of Vapor–Liquid Equilibria of the H_2O + CO_2 + CH_4 Ternary System. J. Chem. Eng. Data 53, 1246–1249.

Regenspurg, S., Wiersberg, T., Brandt, W., Huenges, E., Saadat, A., Schmidt, K., Zimmermann, G., 2010. Geochemical properties of saline geothermal fluids from the in-situ geothermal laboratory Groß Schönebeck (Germany). Chemie der Erde - Geochemistry 70, 3-12.

Sanjuan, B., Millot, R., Dezayes, C., Brach, M., 2010. Main characteristics of the deep geothermal brine (5km) at Soultz-sous-Forêts (France) determined using geochemical and tracer test data. Comptes Rendus Geoscience 342, 546-559.

Savary, V., Berger, G., Dubois, M., Lacharpagne, J.-C., Pages, A., Thibeau, S., Lescanne, M., 2012. The solubility of CO_2+H_2S mixtures in water and 2M NaCl at 120°C and pressures up to 35MPa. International Journal of Greenhouse Gas Control 10, 123-133.

Soreide, I., Whitson, C.H., 1992. Peng-Robinson predictions for hydrocarbons, CO_2, N_2, and H_2S with pure water and NaCl brine. Fluid Phase Equilibria 77, 217-240.

Springer, R.D., Wang, P., Anderko, A., 2015. Modeling the Properties of H_2S/CO_2/Salt/Water Systems in Wide Ranges of Temperature and Pressure. Society of Petroleum Engineers.

Ungerer, P., Wender, A., Demoulin, G., Bourasseau, É., Mougin, P., 2004. Application of Gibbs Ensemble and NPT Monte Carlo Simulation to the Development of Improved Processes for H2S-rich Gases. Molecular Simulation 30, 631-648.

Wang, P., Anderko, A., Young, R.D., 2002. A speciation-based model for mixed-solvent electrolyte systems. Fluid Phase Equilibria 203, 141–176.

Wassiljewa, 1904. Heat conduction in gas mixtures. Physikalische Zeitschrift 5, 737-742.

White, D.E., Ryan, M.A., Armstrong, M.A.C., Gates, J.A., Wood, R.H., 1988. Heat capacity of aqueous magnesium chloride from 349 to 598 K. J. Chem. Eng. Data 33.

Williams, A.E., McKibben, M.A., 1989. A brine interface in the Salton Sea Geothermal System, California: Fluid geochemical and isotopic characteristics. Geochimica et Cosmochimica Acta 53, 1905 - 1920.

Xu, T., Apps, J., Pruess, K., Yamamoto, H., 2007. Numerical modeling of injection and mineral trapping of CO2 with H2S and SO2 in a sandstone formation. Chemical Geology 242, 319-346.

Young, T.F., Smith, M.B., 1954. Thermodynamic Properties of Mixtures of Electrolytes in Aqueous Solutions. The Journal of Physical Chemistry 58, 716-724.

Yusufova, V.D., Pepinov, R.I., Nikolaev, V.A., Guseinov, G.M., 1975. Thermal conductivity of aqueous solutions of NaCl. Journal of engineering physics 29, 1225-1229.

Zezin, D., Driesner, T., Scott, S., Sanchez-Valle, C., Wagner, T., 2014. Volumetric Properties of Mixed Electrolyte Aqueous Solutions at Elevated Temperatures and Pressures. The Systems $CaCl_2$–NaCl–H_2O and $MgCl_2$–NaCl–H_2O to 523.15 K, 70 MPa, and Ionic Strength from (0.1 to 18) mol·kg–1. Journal of Chemical & Engineering Data 59, 2570-2588.

Zhang, H.-L., Chen, G.-H., Han, S.-J., 1997. Viscosity and Density of H_2O + NaCl + $CaCl_2$ and H_2O + KCl + $CaCl_2$ at 298.15 K. J. Chem. Eng. Data 42, 526 - 530.

Ziabakhsh-Ganji, Z., Kooi, H., 2012. An Equation of State for thermodynamic equilibrium of gas mixtures and brines to allow simulation of the effects of impurities in subsurface CO_2 storage. International Journal of Greenhouse Gas Control 11, S21-S34.

Zirrahi, M., Azin, R., Hassanzadeh, H., Moshfeghian, M., 2012. Mutual solubility of CH_4, CO_2, H_2S,

and their mixtures in brine under subsurface disposal conditions. Fluid Phase Equilibria 324, 80-93.

Acknowledgements

The authors gratefully acknowledge the financial support from the German Ministry of Education and Research (BMBF), under the German-Indonesian cooperation project "Sustainability concepts for exploitation of geothermal reservoirs in Indonesia: Capacity building and methodologies for site deployment" (Grant Number 03G0753A), the industry partner Energie Baden Württemberg (EnBW), and the Helmholtz funding program.